

Dynamical quantum correlations after sudden quenches

Utkarsh Mishra,^{1,*} Hadi Cheraghi,² Saeed Mahdavifar,³ R. Jafari,^{4,5,6,†} and Alireza Akbari^{1,7,8,‡}

¹*Asia Pacific Center for Theoretical Physics (APCTP), Pohang, Gyeongbuk, 790-784, Korea*

²*Department of physics, Semnan University, 35195-363, Semnan, Iran*

³*Department of Physics, University of Guilan, 41335-1914, Rasht, Iran*

⁴*Department of Physics, Institute for Advanced Studies in Basic Sciences (IASBS), Zanjan 45137-66731, Iran*

⁵*Department of Physics, University of Gothenburg, SE 412 96 Gothenburg, Sweden*

⁶*Beijing Computational Science Research Center, Beijing 100094, China*

⁷*Department of Physics, POSTECH, Pohang, Gyeongbuk 790-784, Korea*

⁸*Max Planck POSTECH Center for Complex Phase Materials, POSTECH, Pohang 790-784, Korea*

(Dated: July 24, 2018)

We employ the mean-field approach in the fermionic picture of the spin-1/2 XXZ chain to investigate the dynamics of bipartite quantum discord and concurrence under sudden quenching. In the case, when quenching is performed in the anisotropy from an initial value to the critical point, the quantum correlations show periodic cusps in time. Moreover, the first suppression (cusp) in quantum correlations can be explained in terms of the semi-classical picture of quasiparticle propagation. On the other hand, quenching to, as well as away from the criticality point shows that the long time pairwise quantum discord gets enhanced from its initial state. Finally, we show that in the gapped region a quench in the transverse field displays survival of the next nearest-neighbor quantum discord. Our results provide a further insight into the dynamical behavior of quantum correlations and their connections to quantum criticality.

I. INTRODUCTION

Isolated many-body quantum systems, driven away from their equilibrium state, exhibit several interesting features that are important from both fundamental [1–5] and applied perspectives [6–11]. Observing the non-equilibrium dynamics of many-body quantum systems has been made possible in laboratories due to the development of experimental tools in optical lattices, cold atoms, and ion-traps [12–18]. These labs can simulate Hamiltonian dynamics by tuning the control parameters in required ways and can monitor the dynamics of a relatively large number of the constituents. Such experimental setups also allow one to manipulate the system dynamics collectively under the sudden change of engineered Hamiltonian and to record the changes that take place in the dynamics starting from an equilibrium state.

With the success at the experimental front, theoretical study of non-equilibrium dynamics in the closed many-body quantum system has witnessed a new horizon. For example, tracing the influence of equilibrium phase transition in the evolved state, attempts have been made to find universal properties in dynamics similar to the equilibrium phase transitions [3, 19–25]. A specific scenario pertinent to non-equilibrium dynamics in isolated many-body systems is sudden quenching, where system parameters are being switched abruptly, leading to the unitary dynamics [26, 27]. An interesting choice of the quenching protocol is to switch system parameters to,

or close to, the equilibrium critical point. These choices of parameters allow observing certain features in contrast to the quenching away from the critical point. This sharp behaviour can be taken as the signature of criticality [24, 28].

Several static [29–32] and dynamical [26, 27, 33, 34] properties of solid-state systems can be inferred from the investigation of bipartite quantum correlations, such as entanglement [35–37] and quantum discord [38–43]. These quantifiers of quantum correlation can also be realized nowadays experimentally in various setups [14, 18, 44]. The attention towards the study of the quantum correlations, on one hand, is because of their decisive participation in various information processing and computational protocols [45–49]. On the other hand, they have also been relevant to successfully detecting quantum criticality of systems in equilibrium [29–32, 50–54]. Despite several efforts to associate the dynamics of quantum correlation and quantum phase transition, the universal behavior has not yet been fully established. Therefore, it would be necessary to fill the gap by investigating the dynamics of quantum correlations in non-integrable models.

This paper investigates the dynamics of entanglement and quantum discord in a one-dimensional XXZ chain in the presence and absence of a transverse field. To obtain the time-dependent reduced density matrix between two sites, here, we apply a combination of Jordan-Wigner transformation and mean-field approach. This allows us to write the reduced density matrix in terms of two-point fermionic correlation functions, by solving a set of self-consistent equations. This method has been applied to the equilibrium case [55, 56], but to the best of our knowledge, has not been explored for the dynamics. It is known that the XXZ model in the presence of the

*utkarsh.mishra@apctp.org

†jafari@iasbs.ac.ir

‡alireza@apctp.org

transverse field is non-integrable [57], in which two interesting choices of parameters for quenching can be considered. One of the possibilities is quenching the anisotropy parameter, Δ , which can be tuned across different phases connecting gapped to gapless, and then again to gapped ground state. Another choice is quenching the transverse field from different non-integrable limits to an integrable limit. Note that the presence of the transverse field can open a gap in the system of an otherwise gapless phase. With the above choice of quenching parameters in the Hamiltonian, we find several compelling results summarized as:

- (i) We note the occurrence of periodic cusps in the dynamics of quantum discord between nearest neighbor for quenching the anisotropy parameter to the critical point. Furthermore, the first cusp occurs when the quasiparticles are traveling with the group velocity at the critical point.
- (ii) For the general quenching of the anisotropy parameter, the quantum discord increases in time.
- (iii) For a large quenching in the transverse field, the quantum discord between the nearest neighbor spin pairs becomes vanishingly small in the region $0 \leq \Delta < 1$, while quantum discord of the next to next neighbor spin pairs becomes finite, for the same parameters.

The paper is organized as follows. In the next section, we introduce the model and derive an analytical form for the entanglement and the quantum discord. In section III, we present the sudden quench protocol and expression for the time-dependent two-point correlation functions to obtain the reduced density matrix. In Sec. IV A, we present our result on periodic cusp behavior. Sec. IV B presents the dynamics of nearest neighbor concurrence, next to next neighbor and 3rd neighbor quantum discord between the spin pairs for quenching the anisotropy parameter. Section IV C describes the effects on the dynamics of quantum correlations by quenching the magnetic field, and finally, we summarize the results in Sec. V.

II. THE MODEL AND QUANTUM CORRELATIONS

The model: We first outline the main features of the XXZ chain in the absence as well as presence of a transverse magnetic field, respectively. The interaction Hamiltonian of spin-1/2 XXZ Heisenberg chains in a zero field is given by

$$\mathcal{H} = \sum_{j=1}^N J \left(S_j^x S_{j+1}^x + S_j^y S_{j+1}^y + \Delta S_j^z S_{j+1}^z \right), \quad (1)$$

where \mathbf{S}_j is the spin-1/2 operator at j th the site. Here, $J > 0$ denotes the antiferromagnetic exchange coupling,

Δ is the anisotropy parameter, and we consider periodic boundary condition, i.e., $\mathbf{S}_{N+1} = \mathbf{S}_1$. It is well known that at zero temperature the ground state of the XXZ model has three different phases [58]. In which, for the limiting case of $\Delta < -1$, the ground state has a ferromagnetic alignment, accordingly the system shows a first order transition to the gapless Luttinger liquid at $\Delta = -1$, and finally by undergoing a continuous quantum phase transition at $\Delta = 1$, it arrives in the antiferromagnetic phase.

Introducing a transverse magnetic field along the x -direction breaks the $U(1)$ -symmetry and the resulting Hamiltonian becomes non-integrable. To study such a model, it is useful to rotate the spins around y -direction by $\pi/2$, which reshapes the Hamiltonian as [59]

$$\mathcal{H} = \sum_{j=1}^N \left[J(\Delta S_j^x S_{j+1}^x + S_j^y S_{j+1}^y + S_j^z S_{j+1}^z) - h S_j^z \right], \quad (2)$$

with h as the external transverse magnetic field. Further, by applying the Jordan-Wigner transformation, $S_j^+ = a_j^\dagger (e^{i\pi \sum_{l<j} a_l^\dagger a_l})$; $S_j^- = (e^{-i\pi \sum_{l<j} a_l^\dagger a_l}) a_j$, and $S_j^z = a_j^\dagger a_j - \frac{1}{2}$, in Eq. (2), the Hamiltonian is mapped onto the interacting fermionic chain

$$\begin{aligned} \mathcal{H} = \sum_j \left[\frac{J(\Delta - 1)}{4} a_j^\dagger a_{j+1}^\dagger + \frac{J(\Delta + 1)}{4} a_j^\dagger a_{j+1} + \text{H.c.} \right] \\ + \sum_j \left[J \left(a_j^\dagger a_j (a_{j+1}^\dagger a_{j+1} - 1) \right) - h a_j^\dagger a_j \right]. \end{aligned} \quad (3)$$

where $S_j^\pm = \frac{1}{2}(S_j^x \pm iS_j^y)$ are spin raising and lowering operators at site j and $a_j^\dagger(a)$ are the fermionic raising (lowering) operators, respectively. In the next step, we decompose the fermionic interaction terms, $a_j^\dagger a_j a_{j+1}^\dagger a_{j+1}$, using the Wick's theorem, and define the parameters $\Upsilon_{i=1,2,3}$ as an expectation value of the fermionic two-point correlation functions [55],

$$\Upsilon_1 = \overline{\langle a_j^\dagger a_j \rangle}; \quad \Upsilon_2 = \overline{\langle a_j^\dagger a_{j+1} \rangle}; \quad \Upsilon_3 = \overline{\langle a_j^\dagger a_{j+1}^\dagger \rangle}. \quad (4)$$

Here, the expectation values, $\langle \dots \rangle$, are calculated in ground state of the Hamiltonian, and $\overline{\dots}$ is indicating the averaging over the lattice sites. Since the system is translationally invariant, we may move to the Fourier space, $a_j = (1/\sqrt{N}) \sum_q e^{-iqj} a_q$, and employ the Bogoliubov transformation

$$a_q = \cos(\theta_q) \beta_q + i \sin(\theta_q) \beta_{-q}^\dagger, \quad (5)$$

to bring the Hamiltonian in a diagonalized form of

$$\mathcal{H}(\Delta, h) = \sum_q \varepsilon_q(\Delta, h) (\beta_q^\dagger \beta_q - \frac{1}{2}). \quad (6)$$

Thus, the energy spectrum, ε_q , is obtained as

$$\varepsilon_q = \varepsilon_q(\Delta, h) = \sqrt{\mathcal{A}_q^2 + \mathcal{B}_q^2}, \quad (7)$$

with $\tan(2\theta_q) = -\mathcal{B}_q(\Delta, h)/\mathcal{A}_q(\Delta, h)$, where

$$\mathcal{A}_q(\Delta, h) = J \left(\frac{\Delta + 1}{2} - 2\Upsilon_2 \right) \cos(q) + J(2\Upsilon_1 - 1) - h,$$

$$\mathcal{B}_q(\Delta, h) = J \left(2\Upsilon_3 + \frac{\Delta - 1}{2} \right) \sin(q),$$

The above exercise gives the following equations which have to be satisfied self-consistently

$$\begin{aligned} \Upsilon_1(\Delta, h) &= \frac{1}{2} - \frac{1}{2N} \sum_q \frac{\mathcal{A}_q(\Delta, h)}{\varepsilon_q(\Delta, h)}, \\ \Upsilon_2(\Delta, h) &= -\frac{1}{2N} \sum_q \cos(q) \frac{\mathcal{A}_q(\Delta, h)}{\varepsilon_q(\Delta, h)}, \\ \Upsilon_3(\Delta, h) &= \frac{1}{2N} \sum_q \sin(q) \frac{\mathcal{B}_q(\Delta, h)}{\varepsilon_q(\Delta, h)}. \end{aligned} \quad (8)$$

Concurrence: The concurrence is a measure of entanglement between two spins at site i and j . It can be obtained from the corresponding reduced density matrix, ρ_{ij} [35, 36]. In the standard spin basis, we have

$$\rho_{i,j} = \begin{pmatrix} \langle P_i^+ P_j^+ \rangle & \langle P_i^+ S_j^- \rangle & \langle S_i^- P_j^+ \rangle & \langle S_i^- S_j^- \rangle \\ \langle P_i^+ S_j^+ \rangle & \langle P_i^+ P_j^\downarrow \rangle & \langle S_i^- S_j^+ \rangle & \langle S_i^- P_j^\downarrow \rangle \\ \langle S_i^+ P_j^+ \rangle & \langle S_i^+ S_j^- \rangle & \langle P_i^\downarrow P_j^+ \rangle & \langle P_i^\downarrow S_j^- \rangle \\ \langle S_i^+ S_j^+ \rangle & \langle S_i^+ P_j^\downarrow \rangle & \langle P_i^\downarrow S_j^+ \rangle & \langle P_i^\downarrow P_j^\downarrow \rangle \end{pmatrix}, \quad (9)$$

where $P_j^{\uparrow/\downarrow} = \frac{1}{2}\mathbb{I} \pm S_j^z$, and \mathbb{I} represents the 2×2 unit matrix. One can move from the spin-spin correlation of the pairs with the distance m , ($i, j = i + m$), to the fermionic picture with two-point correlation functions, and obtains

$$\rho_{i,i+m} = \begin{pmatrix} X_{i,i+m}^+ & 0 & 0 & -f_{i,i+m}^* \\ 0 & Y_{i,i+m}^+ & Z_{i,i+m}^* & 0 \\ 0 & Z_{i,i+m}^- & Y_{i,i+m}^- & 0 \\ f_{i,i+m} & 0 & 0 & X_{i,i+m}^- \end{pmatrix}. \quad (10)$$

By considering $n_i = a_i^\dagger a_i$ as a fermionic occupation number of the i th mode, we have

$$\begin{aligned} X_{i,i+m}^+ &= \langle n_i n_{i+m} \rangle, \\ Y_{i,i+m}^+ &= \langle n_i (1 - n_{i+m}) \rangle, \\ Y_{i,i+m}^- &= \langle n_{i+m} (1 - n_i) \rangle, \\ Z_{i,i+m} &= \langle a_i^\dagger \left[\prod_{l=i}^{i+m-1} (1 - 2a_l^\dagger a_l) \right] a_{i+m} \rangle, \\ X_{i,i+m}^- &= \langle 1 - n_i - n_{i+m} + n_i n_{i+m} \rangle, \\ f_{i,i+m} &= \langle a_i^\dagger \left[\prod_{l=i}^{i+m-1} (1 - 2a_l^\dagger a_l) \right] a_{i+m}^\dagger \rangle. \end{aligned} \quad (11)$$

Therefore, the concurrence of the density matrix, Eq. (10), is given by

$$C(\rho_{i,i+m}) = \text{Max} \left[0, \Lambda_1, \Lambda_2 \right], \quad (12)$$

with

$$\begin{aligned} \Lambda_1 &= 2 \left(|Z_{i,i+m}| - (X_{i,i+m}^+ X_{i,i+m}^-)^{1/2} \right), \\ \Lambda_2 &= 2 \left(|f_{i,i+m}| - (Y_{i,i+m}^+ Y_{i,i+m}^-)^{1/2} \right). \end{aligned}$$

Quantum discord: In order to capture the quantum correlation present in a bipartite state that are not explored by concurrence, one can also calculate the quantum discord [30]. The quantum discord is defined by difference of total correlation, $\mathcal{I}(\rho_{i,i+m})$, and classical correlation, $\mathcal{C}(\rho_{i,i+m})$, as

$$Q_{i,i+m} = \mathcal{I}(\rho_{i,i+m}) - \mathcal{C}(\rho_{i,i+m}). \quad (13)$$

The total correlation can be calculated as follow

$$\mathcal{I}(\rho_{i,i+m}) = S(\rho_i) + S(\rho_{i+m}) + \sum_{\alpha=0}^3 \lambda_\alpha \log \lambda_\alpha, \quad (14)$$

where λ_α is the eigenvalue of the density matrix $\rho_{i,i+m}$, and

$$S(\rho_i) = - \sum_{\xi=\pm 1} \left[\frac{1 + \xi c_4}{2} \log \left(\frac{1 + \xi c_4}{2} \right) \right]. \quad (15)$$

Here, $c_{i=1,\dots,4}$, are expressed as

$$\begin{aligned} c_{1/2} &= 2Z_{i,i+j} \pm f_{i,i+m}, \\ c_{3/4} &= X_{i,i+j}^+ \pm X_{i,i+j}^- - Y_{i,i+j}^+ \mp Y_{i,i+j}^-. \end{aligned} \quad (16)$$

Note that due to the translation invariance of the original Hamiltonian, the single site density matrices ρ_i and ρ_{i+m} are equal, therefore we have $S(\rho_i) = S(\rho_{i,i+m})$.

The calculation of the classical correlation, $\mathcal{C}(\rho_{i,j})$, requires an optimization over rank-1 local measurements on part B of $\rho_{i,j}$ [38] (here we have taken site j of $\rho_{i,j}$ as part B). A general set of local rank-1 measurement operators, $\{B_0, B_1\}$, can be defined as $B_{k'=0/1} = V \Pi_{k'} V^\dagger$, where $V \in U(2)$ and the projectors $\Pi_{k'}$ are given in the computational basis $|0\rangle \equiv |\uparrow\rangle$ and $|1\rangle \equiv |\downarrow\rangle$. The post measurement outcomes get updated to one of the following states

$$\rho_{k'} = \left(\frac{1}{2} \mathbb{I} + \sum_{j=1}^3 \chi_{k'j} S_j \right) \otimes (V \Pi_{k'} V^\dagger), \quad (17)$$

where the elements of the density matrices are given by

$$\begin{aligned} \chi_{k'i=1,2} &= \frac{c_i \sin \theta \cos \phi}{1 + (-1)^{k'} c_4 \cos \theta} (-1)^{k'}, \\ \chi_{k'3} &= \frac{(-1)^{k'} c_3 \cos \theta + c_4}{1 + (-1)^{k'} c_4 \cos \theta}. \end{aligned} \quad (18)$$

Here the azimuthal angle $\theta \in [0, \pi]$ and the polar angle $\phi \in [0, 2\pi]$ represent a qubit over the Bloch sphere.

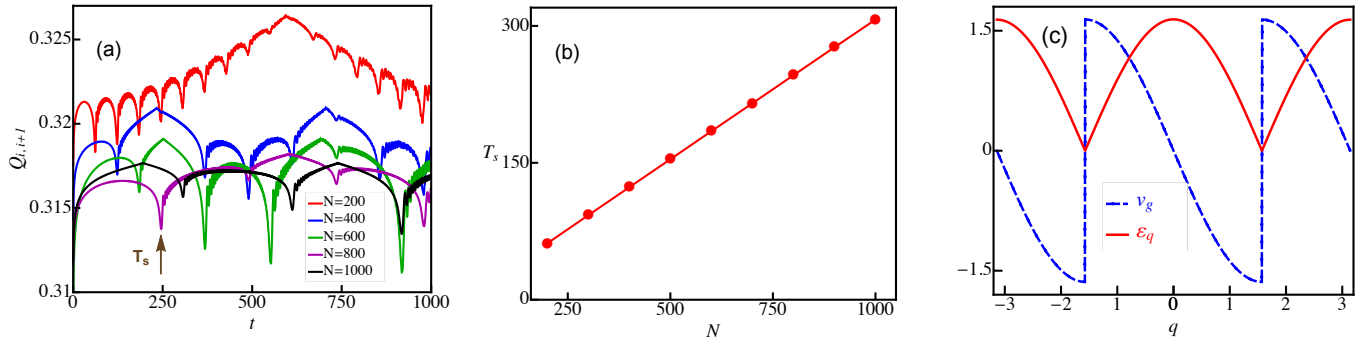


FIG. 1: (Color online) (a) Quantum discord of nearest neighbor spin pairs as a function of time, t , for a quench of anisotropy from $\Delta_I = 0.98$ to the critical point $\Delta_F = \Delta_c = 1$, at zero magnetic field, for different system sizes. For clarifying the position of the first suppression time, T_s , the arrow indicates T_s for the case of $N = 800$. (b) Scaling of first suppression time versus the system sizes N . (c) The ground state energy, ϵ_q , and group velocity of the quasiparticle at the critical point, v_g , at zero magnetic field. The quantum discord is measured in bits while the other quantities are dimensionless for this figure and the rest.

By considering the normalization of the density matrices, $\theta_{k'} = \sqrt{\sum_{j=1}^3 \chi_{k'j}^2}$, we finally arrive to the classical correlation between the spin pairs [30]

$$\mathcal{C}(\rho_{i,i+m}) = \max_{\{B_{k'}\}} \left[S(\rho_i) - \frac{S(\rho_0) + S(\rho_1)}{2} - c_4 \cos \theta \frac{S(\rho_0) - S(\rho_1)}{2} \right], \quad (19)$$

where the von Neumann entropies are identified as

$$S(\rho_{k'}) = - \sum_{\xi=\pm 1} \left[\frac{1 + \xi \theta_{k'}}{2} \log \left(\frac{1 + \xi \theta_{k'}}{2} \right) \right]. \quad (20)$$

Note that the von Neumann entropy of $V \Pi_{k'} V^\dagger$ is zero [30].

III. QUENCH DYNAMICS AND TIME-EVOLVED REDUCED DENSITY MATRIX

For considering a quench dynamics, the system is prepared in the ground state, $|\Psi_0(\Delta_I, h_I)\rangle$, at initial time $t = t_I = 0$, then the parameters (Δ_I, h_I) are switched suddenly to final values (Δ_F, h_F) corresponding to the post-quench Hamiltonian $\mathcal{H}(\Delta_F, h_F)$ at time $t = t_F > 0$. After that, the system is allowed to evolve according to $|\Psi(\Delta_F, h_F)\rangle = e^{-i\mathcal{H}(\Delta_F, h_F)t} |\Psi_0(\Delta_I, h_I)\rangle$. In this case, the self-consistent equations, $\Upsilon_i^I(\Delta_I, h_I)$, are also changed to a new set of the self-consistent equations, $\Upsilon_i^F(\Delta_F, h_F)$. The calculation of two sites reduced density matrix requires knowledge of time dependent two point correlation functions, which can be obtained from

the following equations

$$\begin{aligned} T_m(t) &= \frac{1}{N} \sum_{l=1}^N \langle a_l^\dagger a_{l+m} \rangle \\ &= \frac{1}{N} \sum_{q>0} \cos(qm) \left[1 - \cos(2\theta_q^F) \cos(2\Phi_q) \right. \\ &\quad \left. - \sin(2\theta_q^F) \sin(2\Phi_q) \cos(2\varepsilon_q(\Delta_F, h_F)t) \right], \end{aligned} \quad (21)$$

and

$$\begin{aligned} P_m(t) &= \frac{1}{N} \sum_{l=1}^N \langle a_l^\dagger a_{l+m}^\dagger \rangle \\ &= \frac{1}{N} \sum_{q>0} \sin(qm) \sin(2\Phi_q) \left[\frac{\sin(2\theta_q^F)}{\tan(2\Phi_q)} - \right. \\ &\quad \left. \cos(2\theta_q^F) \cos(2\varepsilon_q(\Delta_F, h_F)t) - i \sin(2\varepsilon_q(\Delta_F, h_F)t) \right], \end{aligned} \quad (22)$$

for a given distance m . Here $\Phi_q = \theta_q^F - \theta_q^I$ is the difference between the Bogoliubov angles diagonalizing the pre-quench and post-quench Hamiltonians, respectively. Note that, here, the expectation values, $\langle \dots \rangle$, are calculated in the time evolve state for the dynamics. Thus, with the help of the above equations, one can calculate quantum correlations both for integrable/nonintegrable cases.

IV. RESULTS AND DISCUSSIONS

Most recently, salient features of dynamics have been linked to the equilibrium quantum phase transitions [4, 22, 60–64]. Specifically, it has been explored how distinct signatures of the equilibrium quantum phase transition is manifested in the dynamics when a system is quenched to the quantum critical point [4, 22, 60]. In a finite system with sudden quenches to a quantum critical point,

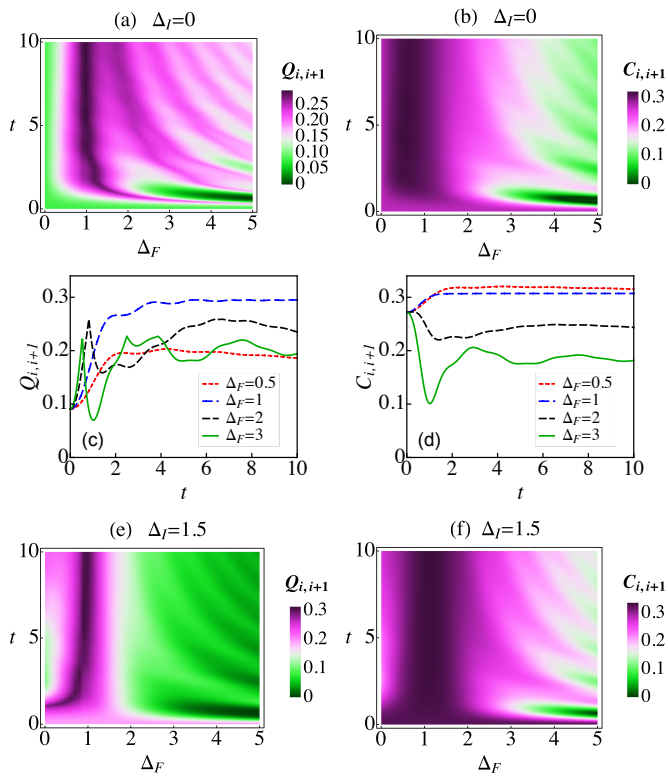


FIG. 2: (Color online) The density plots of quantum discord as a function of anisotropy Δ_F and time for (a) $\Delta_I = 0$ and (e) $\Delta_I = 1.5$. (c) Quantum Discord between the first nearest neighbors as a function of time at zero temperature and zero magnetic field for quench from $\Delta_I = 0$, to $\Delta_F = 0.5, 1, 2, 3$. The density plots of concurrence as a function of anisotropy Δ_F and time for (b) $\Delta_I = 0$. and (f) $\Delta_I = 1.5$. (d) Concurrence between the first nearest neighbors as a function of time at zero temperature and zero magnetic field for quench from $\Delta_I = 0$, to $\Delta_F = 0.5, 1, 2$, and 3 . The concurrence is given in terms of ebits and the dimension of other quantities are dimensionless.

as an example the relaxation of Loschmidt echo, is found to be accelerated [23, 60, 65–69] with periodic recurrence as a signature of criticality [4, 22, 24, 28, 60, 65]. In general, the Loschmidt echo can be related with the quantum discord and the concurrence [27, 70]. In the following subsections, we describe the dynamics of quantum discord under the sudden quenching to the critical point and report the occurrence of periodic structure in its dynamics. Then we analyze two possible scenarios of quenching, namely (i) quenching anisotropy parameter, Δ , in the zero transverse field, and (ii) quenching the transverse field while keeping the fixed value of anisotropy parameter.

A. Periodic suppression in quantum correlations

In Fig. 1(a) the quantum discord of the first neighbor spin pairs has been depicted for quench of the anisotropy

parameter from $\Delta_I = 0.98$ to the critical point, $\Delta_F = \Delta_c = 1$, for different system sizes. As seen in Fig. 1(a), the quantum discord starts from initial non-zero value and gets enhanced in a very short time period, then it keeps exhibiting periodic cusps. The first suppression time, T_s , of the quantum discord has been plotted versus the size of the chain, N , in Fig. 1(b). Examining the Fig. 1(b) shows that T_s is behaving almost linearly with N , $T_s \propto N$. As expectation the scaling ratio is given by half of v_g^{-1} , in which v_g is the group velocity at the critical point defined by [4]

$$v_g = v_g(q) = \left| \frac{\partial \varepsilon_q}{\partial q} \right|. \quad (23)$$

Here ε_q is the energy dispersion, which is presented with its corresponding group velocity, v_g , in the Fig. 1(c). The same feature of the first suppression time, can be extracted from both concurrence of the first neighbor as well as the quantum discord of second and third nearest neighbor spin pairs. The propagation of information in the system can be viewed as quasiparticle wave packets, therefore the first cusp only occurs when the wave packets travel with the group velocity at the critical point. This helps to elucidate the universality of the suppression phenomenon, since the group velocity depends only on the quasiparticle dispersion, and other details such as the initial state and the size of the quench are irrelevant.

B. Quench dynamics under anisotropic parameter: zero magnetic field

Based on the analytical approach (Sec. II), we now analyze the dynamics of quantum discord and concurrence after quenching the anisotropy strength, Δ , from the initial value, Δ_I , to the final point, Δ_F , in the integrable case of magnetic field of the model (Eq. 2) [57]. In this respect, Fig. 2(a) and Fig. 2(e) show the density-representations of quantum discord for the nearest neighbor spin pairs versus time and Δ_F , quenching from $\Delta_I = 0$ and $\Delta_I = 1.5$, respectively. The quantum discord shows its maximum value at $\Delta = \Delta_c = 1$, indicating the presence of critical point [29, 71]. In Fig. 2(c), the pairwise nearest-neighbor quantum discord is plotted as a function of time for quenching from $\Delta_I = 0$, where the initial state of system is in the Luttinger liquid phase, to different final values of $\Delta_F = 0.5, 1, 2$, and 3 . For the quenching within the Luttinger liquid phase, the quantum discord first increases as time increases and then tends to a constant value. For large size and across the critical point quenching, i.e., $\Delta_F = 2$, and $\Delta_F = 3$, the quantum discord rapidly increases with the increment in time to its maximum value, then suddenly drops to its minimum and then increases again to reach the saturated value with irregular oscillations. As a consequence, when quench is performed to the critical point or around it, the quantum discord enhances from the initial value to the saturated value after a long time.

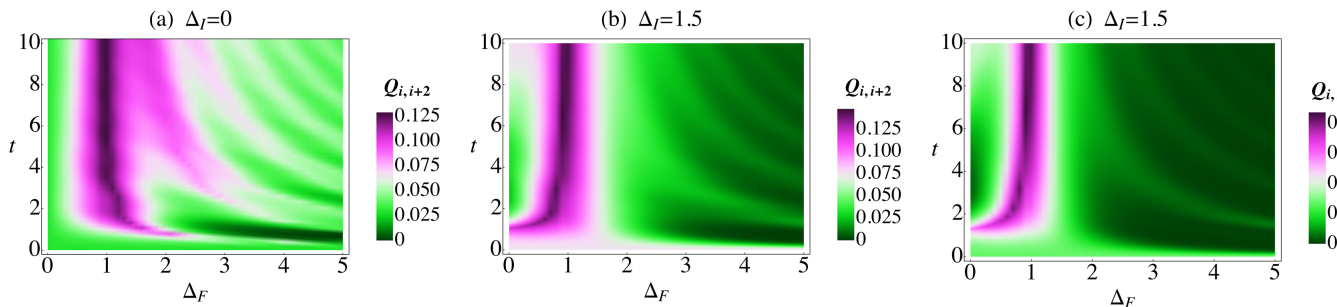


FIG. 3: (Color online) The density plots of quantum discord for a quench from $\Delta_I = 0$ to Δ_F , versus Δ_F and time: between first nearest neighbors (a), and second nearest neighbors (b). (c) represents the density plot of quantum discord between 3rd nearest neighbor spins, for a quench from $\Delta_I = 1.5$ to Δ_F .

In Figs. 2(b and f), we show the density-plots of the concurrence for the nearest neighbor spin pairs as a function of time and final anisotropy, Δ_F , for quenching from $\Delta_I = 0$ and $\Delta_I = 1.5$, respectively. They show, for a quench into the ordered phase and sufficiently far away from the critical point, that the concurrence initially decreases before showing the damped oscillations to its mean value. Note, these oscillations are tiny for smaller size of quench ($|\Delta_I - \Delta_F| < 1$) while becomes prominent for a larger ones. Although the behavior of concurrence for a quench around the critical point is similar to the quantum discord, the maximum of the concurrence does not occur exactly at the critical point. This behavior can be clearly observed from the Fig. 2(d), where the concurrence is plotted as a function of time for the fixed $\Delta_I = 0$ and various Δ_F . Moreover, the entanglement is present only between the nearest neighbor spins, and an increment of time or size of quench do not create entanglement between spin pairs farther than the nearest neighbors. However, as shown in Fig. 3, the quantum discord of the second and third neighboring pairs is nonzero, and as expected, it decreases between the spin pairs beyond the first neighbors. We find that while the maximum of the concurrence does not occur at the critical point, still one can detect the phase-transition via the maximum of quantum discord, even for pairs with higher distances. Even though, the maximum value of the quantum discord between the spin pairs decreases at large distance, the sharpness of the maxima is more prominent in the critical region. Therefore, out of equilibrium dynamics of quantum discord imprints the zero-temperature phase transition.

C. Quench dynamics of non-zero magnetic field

Now we examine the non-equilibrium dynamics of the quantum discord and concurrence by quenching the transverse magnetic field from a pre-quench finite value h_I to a post-quench value $h_F = 0$. The density plot of quantum discord between the nearest and next nearest neighbor spins is depicted in Fig. 4 versus time and

anisotropy parameter for a quench in a different initial magnetic fields: $h_I = 0.2, 0.5, 0.8, 1.4, 1.6$, and 2 . It clearly indicates that the maximum of the quantum discord occurs at the critical point independent of the time. Next we observe that for the small quenches, the quantum discord reaches to a stable value in a long time albeit initial tiny fluctuations, up to a small time scale $t \sim \mathcal{O}(10J^{-1})$, as can be seen from Figs. 4(a-c). Moreover, for a larger difference between the pre and post-quench transverse field, the fluctuations in the quantum discord become prominent around their equilibrium value for a comparatively large time scale $t \sim \mathcal{O}(40J^{-1})$, as seen from Figs. 4(d-f). Thus, as anticipated, the system get driven away from its initial equilibrium state for large size quenches in the transverse field. At this point, it is also interesting to note that the survival of quantum discord between a pair of spins at the nearest neighbor sites depends on the value of the magnetic field, h_I , and the anisotropic parameter. As the magnetic field is increased, the quantum discord decreases for lower values of the anisotropic parameter as can be noticed from Figs. 4(a-f). This behavior has already been reported for the static case in the XXZ model with a transverse field [56]. Here, we extend this behavior for the time dependent case. From Fig. 4(f), we notice a complete depletion of quantum discord for $h_I = 2$ and $0 \leq \Delta \leq 1$ for the entire time. This phenomenon is attributed to the fact that the initial state with a non-zero magnetic field becomes gapped. Therefore, generation of quantum correlations between the pair of nearest neighbor spins become stringent. As anisotropy is increased beyond Δ_c , the quantum discord increases to a non-zero value and remains so throughout the evolution time as depicted in Figs. 4(a-f). This behavior is also similar to the observation for the static case [56]. Figs. 4(g-l) shows the dynamical behavior of quantum discord between spin pairs at the next nearest neighbor distance. The quantum discord between the next nearest neighbor spin pairs show maximum at Δ_c , similar to the quantum discord between nearest neighbor spin pairs shown in figures 4. The dynamics of $Q_{i,i+1}$ and $Q_{i,i+2}$ also shows the imprints of the equilibrium criticality at finite time as can be seen

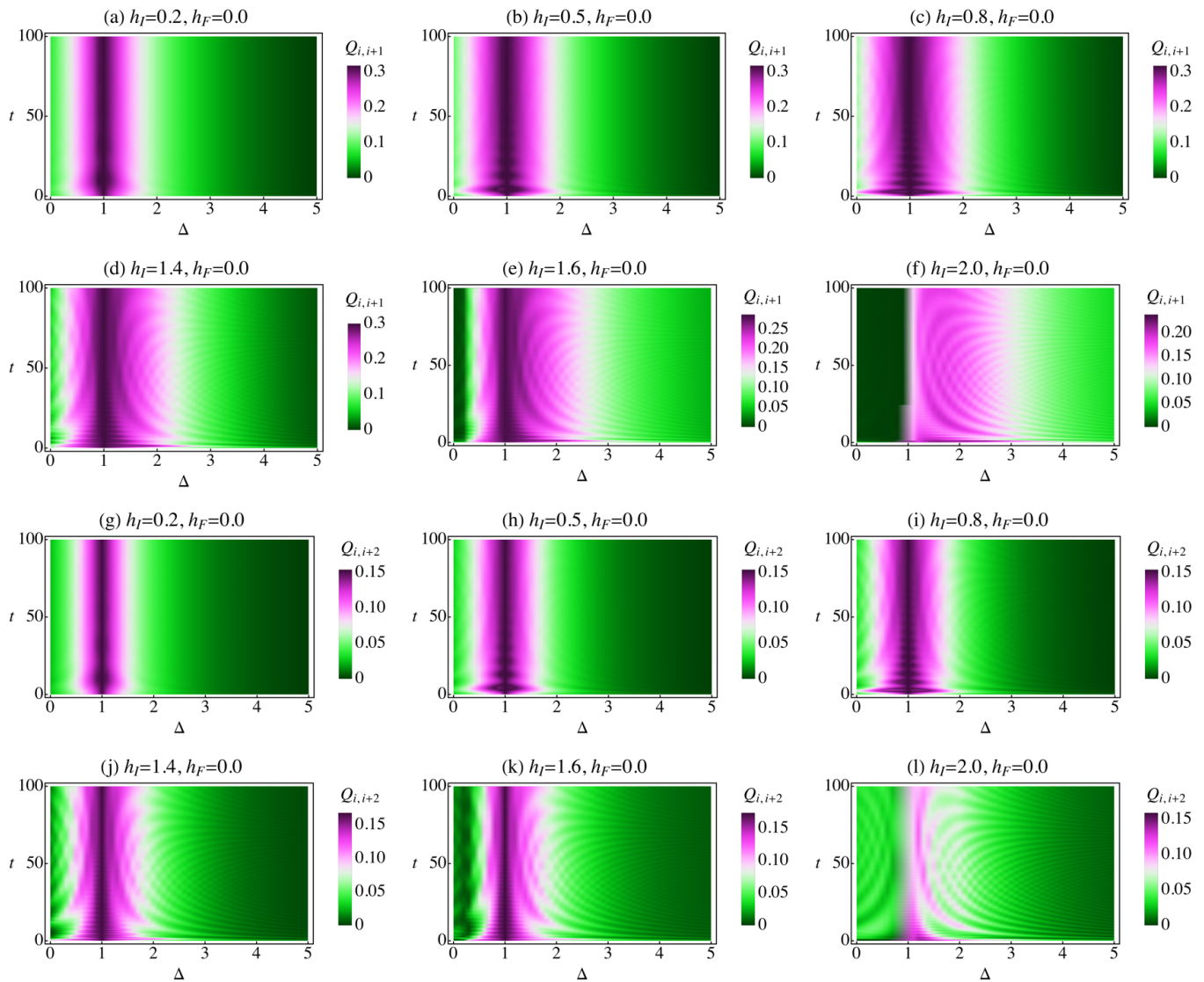


FIG. 4: (Color online) The density plots of quantum discord between first nearest neighbors, $Q_{i,i+1}$, as a function of time, t , and anisotropy, Δ , at zero temperature, for a quench from: (a) $h_I = 0.2$, (b) $h_I = 0.5$, (c) $h_I = 0.8$, (d) $h_I = 1.4$, (e) $h_I = 1.6$, and (f) $h_I = 2$, to $h_F = 0$. The density plots of quantum discord for next nearest neighbor, $Q_{i,i+2}$, for a quench from: (g) $h_I = 0.2$, (h) $h_I = 0.5$, (i) $h_I = 1.8$, (j) $h_I = 1.4$, (k) $h_I = 1.6$, and (l) $h_I = 2$, to $h_F = 0$.

from the distinct dynamics of the quantum discord in the regime $0 \leq \Delta < 1$ and $\Delta > 1$. From Fig. 4(l), it is observed that, unlike the $Q_{i,i+1}$, the depletion of quantum discord, $Q_{i,i+2}$, does not happen for $h_I = 2$ and small anisotropy in long time. Rather, we noticed that $Q_{i,i+2}$ is close to zero at initial time and then evolve to a non-zero value. Thus, though $Q_{i,i+1}$ does not survive in the regime $0 \leq \Delta \leq 1$ for large quenching, $h_I = 2$ and $h_F = 0$, the generation of $Q_{i,i+2}$, takes place in the same parameters. Finally, in Fig. 5, we show the dynamics of nearest neighbor concurrence in the XXZ model by quenching the transverse field. We find that the behavior of nearest neighbor concurrence is similar to the behavior of nearest neighbor quantum discord. For small quenching, Fig. 5(a), the variation in the nearest neighbor concu-

rence with time remains stable to a value close to its equilibrium value. As the quenching strength increases the evolution of concurrence with time is more prominent [see Figs. 5(b-f)]. For a large system size and for a comparatively large quench, e.g., $h_I \geq 1.4$ and $h_F = 0$, the concurrence oscillates in time for a short time scale and then saturates.

V. CONCLUSION

Dynamics of quantum correlations in closed many-body systems show several interesting features. However, their calculation in complex and non-integrable system is still a challenging task. We use the mean-field approach

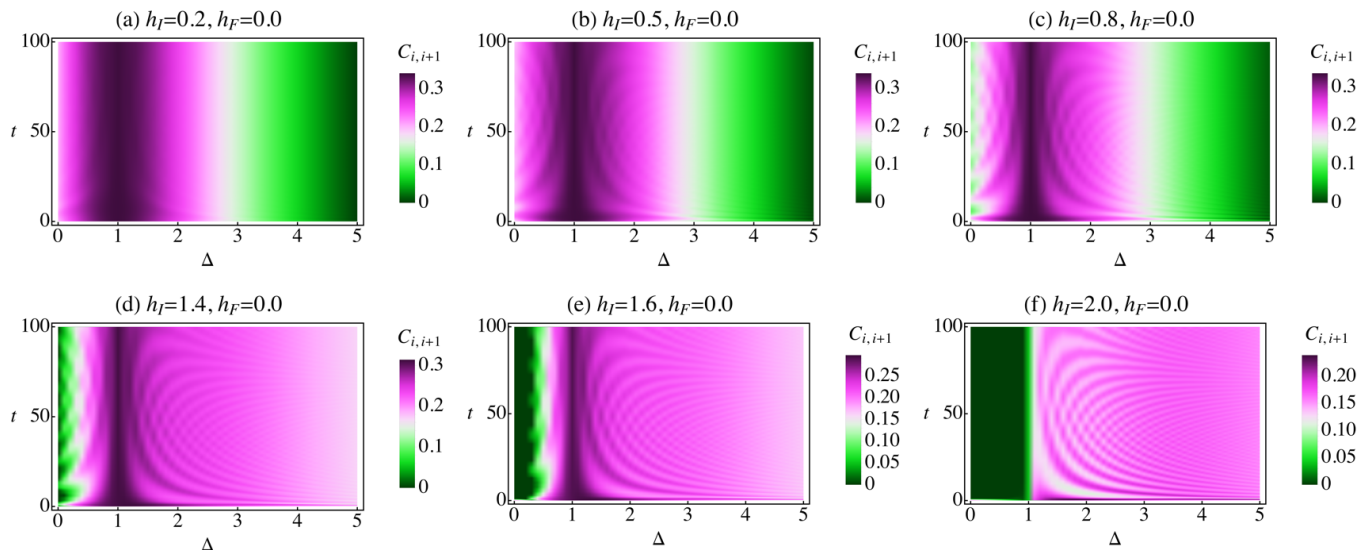


FIG. 5: (Color online) The density plots of concurrence as a function of time, t , and anisotropy, Δ , at zero temperature, for a quench from: (a) $h_I = 0.2$, (b) $h_I = 0.5$, (c) $h_I = 0.8$, (d) $h_I = 1.4$, (e) $h_I = 1.6$, and (f) $h_I = 2$, to $h_F = 0$.

on fermionic picture together with Wick's theorem to diagonalize the Hamiltonian with three self-consistent equations. This enables us to study the dynamics of quantum discord and concurrence between two-sites in spin-1/2 XXZ model in absence and presence of an external transverse magnetic field. The XXZ model is known to host two gapped phases separated by gapless Luttinger liquid phase. When quenching of the anisotropy parameter is performed to the second order quantum critical point from the gapless phases, we observed that the quantum correlations exhibits periodic cusps as a function of time. The occurrence of first cusps corresponds to the suppression of quantum discord and the time of first suppression, T_s , scales as system size, N . Incorporating a semi-classical picture of quasiparticles traveling as a wave-packet, the first suppression time can be predicted by $T_s = N/[2v_g(q)]$, propagating with the group velocity at the critical point, v_g . Thus, we are able to capture the semi-classical picture of information spreading in the quenched XXZ model using an analytical mean-field approach combined with numerical calculation of quantum discord.

In a separate case, we consider quenching of the anisotropy parameter from an initial value, belonging to either gapless or gapped phase, to arbitrary Δ_F . Here, we noticed that when the initial and final values of anisotropy belong to the Luttinger liquid phase, the quantum correlations saturate followed by monotonic increasing behavior with time. On the other hand, when the pre- and post-quench values of the anisotropy parameter are in the different phases, quantum correlations are observed to first decrease to a global minimum before reaching to their mean value following irregular oscillations. This shows that the dynamics of quantum correlations differ when quenching within the disorder phases

and quenching from a disorder phase to an order phase. Moreover, the quantum discord between the first, second and third neighbor spin pairs, finds maxima at the critical point, while from our numerical results, the maximum of nearest neighbor entanglement is shifted from the critical point. Thus, the survival and occurrence of sharp changes in the behavior of quantum discord at the critical point can signal the criticality even in the system away from the equilibrium, while entanglement lack such indicator of criticality in the model. Noticing that the presence of a transverse field breaks the integrability of the XXZ model, we also consider quenching in magnetic field from a non-integrable limit to integrable limit ($h_F = 0$). It is known that the presence of transverse field opens a gap, which may cause a complete depletion of quantum discord between nearest neighbor spins for $0 \leq \Delta < 1$ for large quenching, $|h_I - h_F| > 1.5$. Interestingly, the calculated results of next to next neighbor spin pairs quantum discord, $Q_{i,i+2}$, shows non-zero value in the same regime. It concludes that the present technique can capture silent features of dynamics of quantum correlations in gapped and gapless phases of quantum many body systems.

Acknowledgements

U.M. and A.A. are grateful to R. Fazio, J. Cho, R. Narayanan, and P. Fulde for fruitful discussions, and also thank T. Hiraoka and E. O Colgain for the useful comments. This work is supported through NRF funded by MSIP of Korea (2015R1C1A1A01052411) and (2017R1D1A1B03033465). A.A. acknowledges the Max Planck POSTECH/KOREA Research Initiative (No. 2011-0031558) programs through NRF funded by MSIP

of Korea.

-
- [1] A. Polkovnikov, K. Sengupta, A. Silva, and M. Vengalattore, *Rev. Mod. Phys.* **83**, 863 (2011).
- [2] M. A. Cazalilla and M. Rigol, *New Journal of Physics* **12**, 055006 (2010).
- [3] M. Heyl, *Reports on Progress in Physics* **81**, 054001 (2018).
- [4] J. Häppölä, G. B. Halász, and A. Hama, *Phys. Rev. A* **85**, 032114 (2012).
- [5] Z. Huang and S. Kais, *Phys. Rev. A* **73**, 022339 (2006).
- [6] A. Bayat and S. Bose, *Phys. Rev. A* **81**, 012304 (2010).
- [7] M. Kitagawa and M. Ueda, *Phys. Rev. A* **47**, 5138 (1993).
- [8] J. J. Bollinger, W. M. Itano, D. J. Wineland, and D. J. Heinzen, *Phys. Rev. A* **54**, R4649 (1996).
- [9] A. Bayat, *Phys. Rev. A* **89**, 062302 (2014).
- [10] R. Raussendorf and H. J. Briegel, *Phys. Rev. Lett.* **86**, 5188 (2001).
- [11] A. Bayat and V. Karimipour, *Phys. Rev. A* **75**, 022321 (2007).
- [12] A. Lamacraft and J. Moore., *Ultracold Bosonic and Fermionic Gases* (Elsevier, Oxford, UK, 2012).
- [13] N. Gedik, D.-S. Yang, G. Logvenov, I. Bozovic, and A. H. Zewail, *Science* **316**, 425 (2007).
- [14] O. Mandel, M. Greiner, A. Widera, T. Rom, T. W. Hänsch, and I. Bloch, *Nature* **425**, 937 EP (2003).
- [15] I. Bloch, *Journal of Physics B: Atomic, Molecular and Optical Physics* **38**, S629 (2005).
- [16] P. Treutlein, T. Steinmetz, Y. Colombe, B. Lev, P. Hommelhoff, J. Reichel, M. Greiner, O. Mandel, A. Widera, T. Rom, I. Bloch, and T. Hänsch, *Fortschritte der Physik* **54**, 702 (2006).
- [17] M. Cramer, A. Bernard, N. Fabbri, L. Fallani, C. Fort, S. Rosi, F. Caruso, M. Inguscio, and M. B. Plenio, *Nature Communications* **4**, 2161 EP (2013).
- [18] D. Leibfried, R. Blatt, C. Monroe, and D. Wineland, *Rev. Mod. Phys.* **75**, 281 (2003).
- [19] C. N. Yang and T. D. Lee, *Phys. Rev.* **87**, 404 (1952).
- [20] R. Jafari, *J. Phys. A.: Math. Theor* **49**, 185004 (2016).
- [21] S. Sharma, S. Suzuki, and A. Dutta, *Phys. Rev. B* **92**, 104306 (2015).
- [22] S. Montes and A. Hama, *Phys. Rev. E* **86**, 021101 (2012).
- [23] P. D. Sacramento, *Phys. Rev. E* **90**, 032138 (2014).
- [24] R. Jafari and H. Johannesson, *Phys. Rev. Lett.* **118**, 015701 (2017).
- [25] F. Pollmann, S. Mukerjee, A. G. Green, and J. E. Moore, *Phys. Rev. E* **81**, 020101 (2010).
- [26] A. Mitra, *Annual Review of Condensed Matter Physics* **9**, 245 (2018).
- [27] T. Nag, A. Dutta, and A. Patra, *International Journal of Modern Physics B* **27**, 1345036 (2013).
- [28] R. Jafari and H. Johannesson, *Phys. Rev. B* **96**, 224302 (2017).
- [29] R. Dillenschneider, *Phys. Rev. B* **78**, 224413 (2008).
- [30] M. S. Sarandy, *Phys. Rev. A* **80**, 022108 (2009).
- [31] T. Werlang, C. Trippé, G. A. P. Ribeiro, and G. Rigolin, *Phys. Rev. Lett.* **105**, 095702 (2010).
- [32] Y.-X. Chen and S.-W. Li, *Phys. Rev. A* **81**, 032120 (2010).
- [33] L. Amico, R. Fazio, A. Osterloh, and V. Vedral, *Rev. Mod. Phys.* **80**, 517 (2008).
- [34] J. Eisert, M. Cramer, and M. B. Plenio, *Rev. Mod. Phys.* **82**, 277 (2010).
- [35] S. Hill and W. K. Wootters, *Phys. Rev. Lett.* **78**, 5022 (1997).
- [36] W. K. Wootters, *Phys. Rev. Lett.* **80**, 2245 (1998).
- [37] R. Horodecki, P. Horodecki, M. Horodecki, and K. Horodecki, *Rev. Mod. Phys.* **81**, 865 (2009).
- [38] K. Modi, A. Brodutch, H. Cable, T. Paterek, and V. Vedral, *Rev. Mod. Phys.* **84**, 1655 (2012).
- [39] H. Ollivier and W. H. Zurek, *Phys. Rev. Lett.* **88**, 017901 (2001).
- [40] L. Henderson and V. Vedral, *Journal of Physics A: Mathematical and General* **34**, 6899 (2001).
- [41] J. Oppenheim, M. Horodecki, P. Horodecki, and R. Horodecki, *Phys. Rev. Lett.* **89**, 180402 (2002).
- [42] G. De Chiara and A. Sanpera, *ArXiv e-prints* (2017).
- [43] A. Bera, T. Das, D. Sadhukhan, S. S. Roy, A. Sen(De), and U. Sen, *Reports on Progress in Physics* **81**, 024001 (2018).
- [44] Z.-Y. Sun, S. Liu, H.-L. Huang, D. Zhang, Y.-Y. Wu, J. Xu, B.-F. Zhan, H.-G. Cheng, C.-B. Duan, and B. Wang, *Phys. Rev. A* **90**, 062129 (2014).
- [45] C. H. Bennett, G. Brassard, C. Crépeau, R. Jozsa, A. Peres, and W. K. Wootters, *Phys. Rev. Lett.* **70**, 1895 (1993).
- [46] C. H. Bennett and S. J. Wiesner, *Phys. Rev. Lett.* **69**, 2881 (1992).
- [47] H. J. Briegel, D. E. Browne, W. Dür, R. Raussendorf, and M. Van den Nest, *Nature Physics* **5**, 19 EP (2009).
- [48] A. Datta, A. Shaji, and C. M. Caves, *Phys. Rev. Lett.* **100**, 050502 (2008).
- [49] B. P. Lanyon, M. Barbieri, M. P. Almeida, and A. G. White, *Phys. Rev. Lett.* **101**, 200501 (2008).
- [50] R. Jafari, *Phys. Rev. A* **82**, 052317 (2010).
- [51] B. Tomasello, D. Rossini, A. Hama, and L. Amico, *EPL (Europhysics Letters)* **96**, 27002 (2011).
- [52] B. Tomasello, D. Rossini, A. Hama, and L. Amico, *International Journal of Modern Physics B* **26**, 1243002 (2012).
- [53] T. J. Osborne and M. A. Nielsen, *Phys. Rev. A* **66**, 032110 (2002).
- [54] A. Osterloh, L. Amico, G. Falci, and R. Fazio, *Nature* **416**, 608 EP (2002).
- [55] J.-S. Caux, F. H. L. Essler, and U. Löw, *Phys. Rev. B* **68**, 134431 (2003).
- [56] S. Mahdavifar, S. Mahdavifar, and R. Jafari, *Phys. Rev. A* **96**, 052303 (2017).
- [57] A. Klümper, *Zeitschrift für Physik B Condensed Matter* **91**, 507 (1993).
- [58] M. Takahashi, *Thermodynamics of One-Dimensional Solvable Models* (Cambridge University Press, UK, 1999).
- [59] D. V. Dmitriev, V. Y. Krivnov, and A. A. Ovchinnikov, *Phys. Rev. B* **65**, 172409 (2002).
- [60] H. T. Quan, Z. Song, X. F. Liu, P. Zanardi, and C. P. Sun, *Phys. Rev. Lett.* **96**, 140604 (2006).
- [61] M. Heyl, A. Polkovnikov, and S. Kehrein, *Phys. Rev.*

- Lett. **110**, 135704 (2013).
- [62] S. Campbell, Phys. Rev. B **94**, 184403 (2016).
- [63] R. Dornier, J. Goold, C. Cormick, M. Paternostro, and V. Vedral, Phys. Rev. Lett. **109**, 160601 (2012).
- [64] C. Karrasch and D. Schuricht, Phys. Rev. B **87**, 195104 (2013).
- [65] Z.-G. Yuan, P. Zhang, and S.-S. Li, Phys. Rev. A **76**, 042118 (2007).
- [66] J. Zhang, F. M. Cucchietti, C. M. Chandrashekar, M. Laforest, C. A. Ryan, M. Ditty, A. Hubbard, J. K. Gamble, and R. Laflamme, Phys. Rev. A **79**, 012305 (2009).
- [67] D. Rossini, T. Calarco, V. Giovannetti, S. Montangero, and R. Fazio, Phys. Rev. A **75**, 032333 (2007).
- [68] D. Rossini, T. Calarco, V. Giovannetti, S. Montangero, and R. Fazio, Journal of Physics A: Mathematical and Theoretical **40**, 8033 (2007).
- [69] S. Sharma and A. Rajak, Journal of Statistical Mechanics: Theory and Experiment **2012**, P08005 (2012).
- [70] S. Mukherjee and T. Nag, ArXiv e-prints (2018).
- [71] J.-M. Cai, Z.-W. Zhou, and G.-C. Guo, Physics Letters A **352**, 196 (2006).